

## ***SIMULATION OF THE VUV SPECTRA FROM THE REVERSED FIELD-PINCH EXTRAP T2R PLASMA. Z-EFF DISCREPANCY ANALYSIS ON THE JET PLASMA.***

*V. Stancalie, V. Pais, A. Mihailescu, A.R.D. Chelmus*

*National Institute for Laser, Plasma and Radiation Physics, Magurele*

### **1. Introduction**

The work undertaken in 2005 has been devoted to “plasma diagnostics” and “spectroscopy related to better understanding of plasma characteristics for improved concept”, the specific ITER and JET objectives related to the establishment of databases needed for the interpretation of diagnostics or experiments (atomic data for spectroscopy). On the basis of selected experiments, results refer to the following specific milestones: *a)* checking/reviewing what was done before in evaluating Gaunt factors for the refinement of Zeff evaluation in the JET plasma; *b)* uncertainties in the fundamental component rate-coefficients and their consequences on the spectral identification and interpretation; *c)* accuracy of the atomic data calculation for complex atoms ; *d)* development of web services for remote data access and distributed applications, *e)* recombination and bremsstrahlung power loss in the Extrap T2R reverse field pinch; *f)* radiated power and impurity concentrations in the Extrap T2R reverse field pinch.

### **2. Results**

Under co-operation with Task Force D and Core-Spectroscopy Group, as part of the JET 2004 Workprogramme, most part of the work has been oriented toward contributing on outstanding issue of discrepancies in Zeff measurements. With this aim the computational implementation incorporated TEC Web Umbrella Interface to access experimental measurements used into theoretical calculation of the line integrated intensity from visible bremsstrahlung emission. These data were then been considered to probe possible reasons that may contribute to resolving the discrepancy between Zeff as measured by the charge exchange system and the visible continuum spectrum.

During 2005 the work can be summarized as follows:

**2.1. Objective 1.:** Reconciliation between the two methods (VB and CXS) of measuring Zeff on JET and technique for keeping both diagnostics system synchronized

#### **2.1.1. Achievements**

- New method to calculate Gaunt factor for the refinement of Zeff evaluation on the fusion plasmas [1, 2] (Milestone completed).

Following previous analysis, Gaunt factors are affected by errors, which can be seen in Zeff discrepancies. The main interest was concerning with any evidence of different

temperature scaling for free-free Gaunt factor. Assuming that  $T_e$ -profiles, and more importantly, their mapping on flux coordinates are correctly calculated, there may possible be a different edge  $T_e$  – dependence in the Gaunt factors. A script file has been constructed which gives line of sight integrated intensity from the KS3 spectrometer (horizontal and vertical visible bremsstrahlung signals). The file gets data from TEC Web immediately that the plasma pulse is processed. Then the line of sight integrated intensity is used to output Gaunt factors to be compared with theoretical value. Calculation was based on the definition of the effective oscillator strength,  $f_{\text{eff}}$ , averaged over continuous spectrum as function of the averaged excitation energy,  $E_s$  (Figure 1) Using the Sturmian representation of the Coulomb Green's function in energy, is possible to output free-free and free-bound Gaunt factors in a consistent way. Then results are compared with previously reported values. Application referred to  $C^{2+}$ ,  $W^{18+}$  and  $Ar^{14+}$ . Calculations were been performed in intermediate  $jk$  coupling scheme.

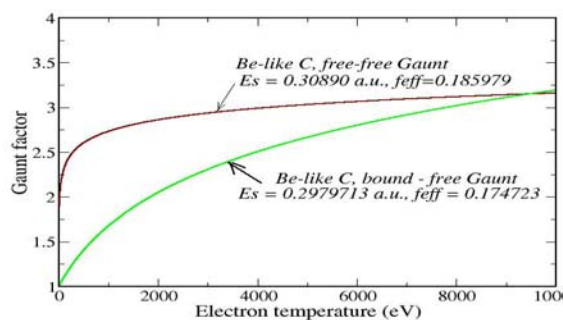


Figure 1. Gaunt factors for  $C^{2+}$  at given photon energy,  $E_s$ , in atomic units, versus  $T_e$  in eV.

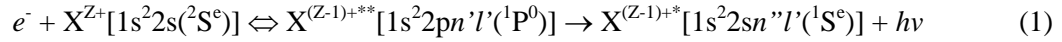
Table 1. The effective oscillator strengths,  $f_{\text{eff}}$ , averaged over continuum for  $W^{18+}$  and  $Ar^{14+}$ . Continuum quantum numbers  $n_s$  ranges from  $n_1$  to 15.

Ion	transition	$f_{\text{eff}}(n_1)$	$f_{\text{eff}}(n_1)$
$W^{18+}$	$[Xe]6p_{3/2}n_1h \rightarrow 6s_{1/2}n_s g$	$k=7/2$	$k=9/2$
	$n_1 = 6$	1.028552	0.411421
	$= 7$	1.296603	0.518641
	$= 8$	0.292346	0.116938
$Ar^{14+}$	$[Xe]2p_{3/2}n_1d \rightarrow 2s_{1/2}n_s p$	$k=1/2$	$k=3/2$
	$n_1 = 3$	0.126883	0.063441
	$= 4$	0.088255	0.044127

- Uncertainties in the fundamental rate-coefficients [3, 4] (Milestone completed)

Results draw attention to the role of di-electronic recombination process (DR) in plasma spectroscopy and the accuracy of atomic data provided when the question under investigation is the calculated line intensity for spectroscopic analysis. The method for atomic rates calculation via ADAS is based on multielectron configuration structure (Cowan structure code), distorted-wave cross sections, close-coupling and incipient R-matrix technique. These rates, necessary for spectral identifications, also form the major frame of collisional-radiative modes in plasmas. The effective coefficients depend on many individual reactions. Dielectronic recombination (DR) is a dominant electron-ion recombination process that should be more accurately considered in ADAS. The total rate of recombination in plasma is obtained from all doubly excited states and the process is particularly important in high temperature plasmas since whole Rydberg series of doubly excited states can contribute. In the calculation of DR rates, there is still uncertainty in the best way of including radiation damping. The allowance for radiative decay can produce important changes for calculated excitation rate

coefficients. For highly ionized ions in an isoelectronic sequence the autoionisation probabilities are approximately independent on  $Z$  but the radiative transition probabilities is proportional to  $Z^4$  (for transitions involving a change of principal quantum number). Reported results [3] demonstrated that the interaction with radiation field might be considered to give additional channels in the collision problems. The basic process of interest is:



where  $X^{Z+}$  signifies the Li-like ion (as an example) of nuclear charge  $Z$  in its ground state, and  $X^{(Z-1)+**}$  is the doubly excited state of corresponding Be-like ion of nuclear charge  $(Z-1)$ . This state can decay by radiative transition to other excited state  $X^{(Z-1)+*}$ . From equation (1) we see that, while radiative transition probability,  $\Gamma^r$ , is approximately independent of  $n'$  for high  $n'$ , the autoionisation width,  $\Gamma^a$ , behaves as  $\Gamma^a = \frac{a}{n'^3}$ , where  $a$  is some constant which depends on the Rydberg series but not on  $n'$ . Hence for sufficiently high  $n'$  Eq. (1) will hold. In this case it is necessary to take account of the radiation field in calculating the autoionization process. This means that a simple use of perturbation theory is not appropriate.

Our approach is to consider the reverse process in the equation (1) corresponding to single-photon ionization. This transition should be studied throughout resonant Rydberg series in a region where the autoionizing and radiative rates are comparable in size. We will consider a laser field of angular frequency  $\omega = \Delta E$  (the transition energy corresponding to the initial unperturbed – field free- Rydberg states) and an intensity given (as an appropriate guess) by the electric field strength of the  $2s-2p$  core transition in Li-like ion. It is analyzed the situation when two excited Rydberg states are resonantly coupled by an intense, monochromatic, monomode, linearly polarized laser field. In order to understand the general features of these structures embedded by the field, we have used a model that retains the essential ingredients of *the full R-matrix Floquet calculation*, namely, a bound state coupled nonperturbatively by the field to an autoionizing state and to the continuum. The standard R-matrix program has been used to calculate the field-free atomic states, including a full description of the electron-electron correlation. The atomic system is then dressed by a monochromatic, linearly polarized laser field of frequency  $\omega$  and intensity  $I$ . The time-dependent Schrödinger equation is solved by expanding the wavefunction as a Floquet-Fourier series. This yields a block structure of the Hamiltonian, each block corresponding to the absorption or emission of a specific number of photons. By diagonalizing the Hamiltonian matrix in the inner region in length gauge, we obtain the R-matrix at the boundary of the box (radius  $a$ ). This matrix, transformed from the length to the velocity gauge, is propagated over an outer region to a radius  $a'$ , where the long range interactions are small. At this radius, we match the R-matrix with an asymptotic expansion of the wave function to obtain the energy  $E$  and width  $\Gamma$  of the system as a complex quasi-energy  $E_F = E - i\Gamma/2$ .

We illustrate the method studying the motion of the complex energies in the complex plane as function of the field intensity for different field frequencies and atomic parameters. Most interesting is the critical region where a crossing (or an avoiding crossing) of trajectories occurs. The motion of the trajectories in the complex plane shows different features of the coupled states. Close to Laser Induced Degenerate State (LIDS) position, LIDS frequency for fixed intensity can be predicted as complex trajectories with a real part avoided crossing

and an imaginary part crossing switch to having a real part crossing and an imaginary part avoided crossing as  $\omega$  passes through LIDS frequency. In all curves where we are really closed to the LIDS position, the imaginary part of the bound state energy, i.e. the width, increased rapidly with intensity while, the real part remained essentially constant. Also, the width of autoionizing state decreased rapidly from its zero field value and its real part of the energy also remained essentially constant. Figure 2 presents the motion in the complex plane [4] of the quasi energies belonging to  $1s^22s5s$  and  $1s^22p7s$  states in  $C^{3+}$ . For each frequency, there are two curves, one connected adiabatically to the 'bound' and the other to the autoionizing state.

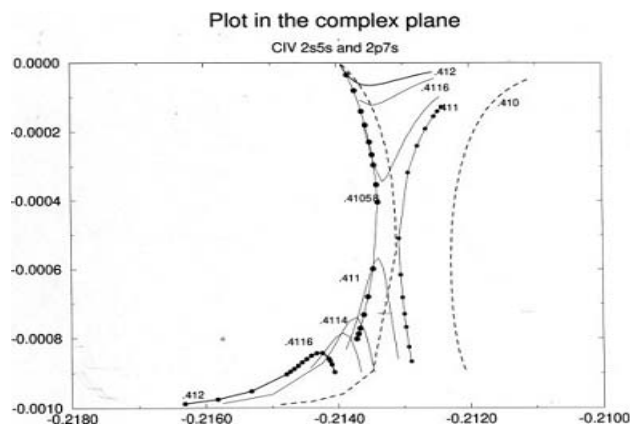


Figure 2. Trajectories of the complex energies of  $1s^22s5s(^1S^e)$  and  $1s^22p7s(^1P^0)$  states as function of field intensity and frequency. For each frequency, there are two curves, one connected adiabatically to the 'bound' and the other to the autoionizing state. The intensity is varied from 0.0 to  $510^{13} \text{ W cm}^{-2}$ . The small dots give intensity in steps of  $5 \times 10^{11} \text{ W cm}^{-2}$ . At very small detunings (e.g.  $\omega = 412$ ), the curve connected to the autoionizing state increases in width with intensity, while the bound state is "trapped" closed to the real axis. For intermediate detunings, two structures are visible, about which the curves of the 'bound' states and of the autoionizing state exchange their roles. The atomic units are used and the energy scale is chosen such that ground states energy is set to zero.

We have calculated the autoionization probabilities, radiative transition probabilities and the influence of damping effect on dielectronic recombination of Li-like into Be-like Al and C ions for  $\Delta n = n' - n'' = 0, 2$  in the Equation 1. In all these calculations, the imaginary part of each quasi-energy in the complex plane, for each field intensity at given field frequency, gives the quantity  $(\Gamma^a + \Gamma^{field})$ , where  $\Gamma^{field}$  is an additional term, signifying the correction due to the interaction with the ion field ( $\Gamma^a = -2 \times \text{Im}(E)$ ).

- Accuracy of the atomic data calculation for complex atoms [5-8] (Milestone to be continued in 2006)

The field of electron-ion collision studies has reached a level of maturity where both, in recombination and ionization, total cross sections are investigated with excellent precision. In this case is usually necessary to have an accurate representation of several target states and the energy gap between them. In the R-matrix method the accuracy of calculation is therefore crucially dependent on the representation of the problem in the inner region. In this region, the number of configurations that have to be generated in a scattering calculation is the number of target configurations *times* the number of continuum orbitals summed over all target states[5]. The primary purpose of this work has been to output energy levels and collision strengths for complex atoms as Co and Ni using the R-matrix code [6]. These species are complicated by having open 3d shells, which gives rise to large numbers of low-lying target

energy levels, whose associated channels are strongly coupled. In electron-impact excitation of these complex atoms, large number of target states are required both to allow for coupling between levels, and to obtain accurate atomic structure via a large configuration –interaction basis. The importance of the contribution from resonances to the rate coefficients for many transitions makes the R-matrix method the optimal close-coupling theory to use. New algorithms to treat  $d$  –shells efficiently, and associated computer codes for implement them, have been developed at Queen’s University of Belfast. These codes have been used to output target states for  $Co^{3+}$ ,  $1s^2 2s^2 2p^6 3s^2 3p^6 3d^6$  configuration. Eight orthogonal one-electron orbitals  $1s, 2s, 2p, 3s, 3p, 3d, 4s, 4p$  were used in our work. The configuration interaction structure code CIV3 was used. The radial orbitals  $1s, 2s, 2p, 3s, 3p, 3d$  were taken from Clementi and Roetti and the rest were optimized in CIV3. The calculated energy of the states relative to the ground agreed well with observed values. Our results are believed to be the first calculation for this system.

High particle and energy fluxes in future fusion experiments demand the investigation of materials for plasma facing components. A promising alternative to the present frequently used low-Z materials carbon and beryllium is tungsten. Due to the high temperature in the plasma, the tungsten ions reach high ionization stages and the radiation of the element occurs mainly in the far ultraviolet (VUV), extreme ultraviolet (EUV) and X ray regions. There have been many measurements of particular lines and many theoretical predictions of transitions. Our work[7] presents collision data for Zn-like W ion, transitions of type  $[Ar]3d^{10} 4s nl \rightarrow [Ar]4s n'l'$  with  $n, n' = 4, 5$  and  $l, l' = 0, 1, 2, 3$ , for  $\Delta J = 0, 1$ . The configurations that have been used are tagged as follows: 1-  $[Ar] 3d^{10} 4s^2$ , 2-  $[Ar] 3d^{10} 4s 4p$ , 3-  $[Ar] 3d^{10} 4s 4d$ , 4-  $[Ar] 3d^{10} 4s 4f$ , 5-  $[Ar] 3d^{10} 4s 5s$ , 6-  $[Ar] 3d^{10} 4s 5p$ , 7-  $[Ar] 3d^{10} 4s 5d$ , 8-  $[Ar] 3d^{10} 4s 5f$ . The atomic structure code of Cowan was used to output the plane-wave-Born collision strengths. State Energies are given in Table 2. Selected collision strengths are presented in Table 3.

Table 2. Zn-like W state energies in  $1000cm^{-1}$  units.

Config.	State	Energy level	J	Config	State	Energy level	J
1	$[Ar] 3d^{10} 4s^2$	0	0				
2	$[Ar] 3d^{10} 4s 4p$	6.6887 <sup>02</sup>	0	5	$[Ar] 3d^{10} 4s 5s$	7.6870 <sup>03</sup>	0
2	$[Ar] 3d^{10} 4s 4p$	7.2742 <sup>02</sup>	1	6	$[Ar] 3d^{10} 4s 5p$	8.0215 <sup>03</sup>	0
2	$[Ar] 3d^{10} 4s 4p$	1.5035 <sup>03</sup>	2	6	$[Ar] 3d^{10} 4s 5p$	8.0286 <sup>03</sup>	1
2	$[Ar] 3d^{10} 4s 4p$	1.6518 <sup>03</sup>	1	6	$[Ar] 3d^{10} 4s 5p$	8.4109 <sup>03</sup>	2
3	$[Ar] 3d^{10} 4s 4d$	2.7624 <sup>03</sup>	1	6	$[Ar] 3d^{10} 4s 5p$	8.4258 <sup>03</sup>	1
3	$[Ar] 3d^{10} 4s 4d$	2.7892 <sup>03</sup>	2	7	$[Ar] 3d^{10} 4s 5d$	8.9875 <sup>03</sup>	1
3	$[Ar] 3d^{10} 4s 4d$	2.9384 <sup>03</sup>	3	7	$[Ar] 3d^{10} 4s 5d$	8.9916 <sup>03</sup>	2
3	$[Ar] 3d^{10} 4s 4d$	3.0033 <sup>03</sup>	2	7	$[Ar] 3d^{10} 4s 5d$	9.0721 <sup>03</sup>	3
4	$[Ar] 3d^{10} 4s 4f$	4.2801 <sup>03</sup>	2	7	$[Ar] 3d^{10} 4s 5d$	9.0792 <sup>03</sup>	2
4	$[Ar] 3d^{10} 4s 4f$	4.2917 <sup>03</sup>	3	8	$[Ar] 3d^{10} 4s 5f$	9.6612 <sup>03</sup>	2
4	$[Ar] 3d^{10} 4s 4f$	4.3293 <sup>03</sup>	4	8	$[Ar] 3d^{10} 4s 5f$	9.6639 <sup>03</sup>	3
4	$[Ar] 3d^{10} 4s 4f$	4.3636 <sup>03</sup>	3	8	$[Ar] 3d^{10} 4s 5f$	9.6870 <sup>03</sup>	4
5	$[Ar] 3d^{10} 4s 5s$	7.6324 <sup>03</sup>	1	8	$[Ar] 3d^{10} 4s 5f$	9.6918 <sup>03</sup>	3

As to what concerns the collision strengths data, the basic code output consists of the values of the momentum transfer and also for each spectrum line (or rather each  $J$ - $J'$  excitation) the program provides values of the weighted generalized oscillator strength and those of the weighted transition probability  $gA$ . Accompanying the collision strengths ( $\Omega$ ) are the excitation rate coefficients computed from the modified  $\Omega$  by integration over Maxwellian distribution, at electron temperatures ranging from  $T_e=5$  to 10000 eV and Table 4 presents a selection of these coefficients at different temperature.

Table 3. Zn-like W ion, selected total collision strengths.

Trans.	T=500 (eV)	700 (eV)	1000 (eV)	1500 (eV)	2000 (eV)	3000 (eV)
7-4	1.1147 <sup>-01</sup>	1.2189 <sup>-01</sup>	1.3290 <sup>-01</sup>	1.4458 <sup>-01</sup>	1.5676 <sup>-01</sup>	1.6932 <sup>-01</sup>
3-6	1.4418 <sup>-01</sup>	1.6041 <sup>-01</sup>	1.7758 <sup>-01</sup>	1.9559 <sup>-01</sup>	2.1428 <sup>-01</sup>	2.3354 <sup>-01</sup>
2-6	2.0115 <sup>-01</sup>	2.0568 <sup>-01</sup>	2.0973 <sup>-01</sup>	2.1331 <sup>-01</sup>	2.1645 <sup>-01</sup>	2.1921 <sup>-01</sup>
3-7	3.7936 <sup>-01</sup>	3.8690 <sup>-01</sup>	3.9362 <sup>-01</sup>	3.9958 <sup>-01</sup>	4.0485 <sup>-01</sup>	4.0946 <sup>-01</sup>
4-8	5.2510 <sup>-01</sup>	5.3330 <sup>-01</sup>	5.4064 <sup>-01</sup>	5.4722 <sup>-01</sup>	5.5305 <sup>-01</sup>	5.5808 <sup>-01</sup>
3-8	6.0714 <sup>-01</sup>	6.7833 <sup>-01</sup>	7.5324 <sup>-01</sup>	8.3140 <sup>-01</sup>	9.1221 <sup>-01</sup>	9.9522 <sup>-01</sup>
1-2	1.3627 <sup>00</sup>	1.4225 <sup>00</sup>	1.4834 <sup>00</sup>	1.5451 <sup>00</sup>	1.6075 <sup>00</sup>	1.67039 <sup>00</sup>
3-2	5.0728 <sup>00</sup>	5.3078 <sup>00</sup>	5.5475 <sup>00</sup>	5.7908 <sup>00</sup>	6.0368 <sup>00</sup>	6.2846 <sup>00</sup>
3-4	5.9981 <sup>00</sup>	6.2667 <sup>00</sup>	6.5405 <sup>00</sup>	6.8183 <sup>00</sup>	7.0988 <sup>00</sup>	7.3814 <sup>00</sup>
5-6	7.0660 <sup>00</sup>	7.3957 <sup>00</sup>	7.7319 <sup>00</sup>	8.0728 <sup>00</sup>	8.4177 <sup>00</sup>	8.7653 <sup>00</sup>
7-6	1.3474 <sup>01</sup>	1.4153 <sup>01</sup>	1.4846 <sup>01</sup>	1.5550 <sup>01</sup>	1.6263 <sup>01</sup>	1.6981 <sup>01</sup>
7-8	1.9557 <sup>01</sup>	2.0504 <sup>01</sup>	2.1471 <sup>01</sup>	2.2452 <sup>01</sup>	2.3444 <sup>01</sup>	2.4444 <sup>01</sup>

Table 4. Zn-like W ion, selected excitation rate coefficients in  $\text{cm}^3\text{s}^{-1}$  units.

Trans.	T=500 (eV)	700 (eV)	1000 (eV)	1500 (eV)	2000 (eV)	3000 (eV)
3-6	1.2840 <sup>-12</sup>	1.7326 <sup>-12</sup>	2.1718 <sup>-12</sup>	2.6129 <sup>-12</sup>	2.8880 <sup>-12</sup>	3.2191 <sup>-12</sup>
7-4	1.4907 <sup>-12</sup>	1.8765 <sup>-12</sup>	2.2056 <sup>-12</sup>	2.4863 <sup>-12</sup>	2.6360 <sup>-12</sup>	2.7889 <sup>-12</sup>
2-6	1.7380 <sup>-12</sup>	2.4687 <sup>-12</sup>	3.0882 <sup>-12</sup>	3.5070 <sup>-12</sup>	3.6227 <sup>-12</sup>	3.5807 <sup>-12</sup>
3-8	3.1504 <sup>-12</sup>	4.7189 <sup>-12</sup>	6.4201 <sup>-12</sup>	8.2757 <sup>-12</sup>	9.5030 <sup>-12</sup>	1.1060 <sup>-11</sup>
4-8	7.5217 <sup>-12</sup>	9.4662 <sup>-12</sup>	1.0778 <sup>-11</sup>	1.1318 <sup>-11</sup>	1.1201 <sup>-11</sup>	1.0552 <sup>-11</sup>
3-7	7.9974 <sup>-12</sup>	1.0680 <sup>-11</sup>	1.2742 <sup>-11</sup>	1.3921 <sup>-11</sup>	1.4084 <sup>-11</sup>	1.3605 <sup>-11</sup>
1-2	6.5434 <sup>-11</sup>	6.4825 <sup>-11</sup>	6.2598 <sup>-11</sup>	5.8835 <sup>-11</sup>	5.5700 <sup>-11</sup>	5.0957 <sup>-11</sup>
3-2	2.2196 <sup>-10</sup>	2.2367 <sup>-10</sup>	2.1904 <sup>-10</sup>	2.0852 <sup>-10</sup>	1.9891 <sup>-10</sup>	1.8366 <sup>-10</sup>
3-4	2.8242 <sup>-10</sup>	2.8088 <sup>-10</sup>	2.7216 <sup>-10</sup>	2.5664 <sup>-10</sup>	2.4345 <sup>-10</sup>	2.2329 <sup>-10</sup>
5-6	4.7198 <sup>-10</sup>	4.4944 <sup>-10</sup>	4.2119 <sup>-10</sup>	3.8621 <sup>-10</sup>	3.6067 <sup>-10</sup>	3.2484 <sup>-10</sup>
7-6	8.4227 <sup>-10</sup>	8.1237 <sup>-10</sup>	7.7026 <sup>-10</sup>	7.1442 <sup>-10</sup>	6.7196 <sup>-10</sup>	6.1063 <sup>-10</sup>
7-8	1.3094 <sup>-09</sup>	1.2500 <sup>-09</sup>	1.1744 <sup>-09</sup>	1.0797 <sup>-09</sup>	1.0101 <sup>-09</sup>	9.1177 <sup>-10</sup>

Additionally, the atomic data for tungsten ions belonging to Ba-like, Ca-like, Hf-like, Sr-like iso-electronic sequences have been provided [8].



- Using web services for remote data access and distributed applications [9] (Milestone to be continued in 2006).

Research on fusion requires effective collaboration between members who are not co-located in time and space. Remote computing environments are needed to share information between experts in nuclear fusion research from institutes and universities, distributed throughout one or more countries. The amount of available data is increasing continuously, which requires new techniques for compression, archiving and retrieval. Recently, hybrid data acquisition systems with MDSplus have been proposed to acquire data and then archive it onto a hard disk. Our work presented [9] the possibility of using web services to implement a collaborative environment assisting the remote participation for fusion research. Before choosing this approach other alternatives were considered, like Remote Procedure Call (RPC) and Common Object Request Broker Architecture (CORBA). The main advantages of using the web service approach are the security features that can be implemented inside the service or in a service independent manner, using mechanisms provided by the web server, and the possibility of using standard Hyper Text Transfer Protocol (HTTP) proxies.

A web service has been developed (Figure 3) that offers processing routines for standard spectroscopic data. Radial components of the hydrogenic and Coulomb Green's function in its Sturmian representation are integrated numerically based on other web services where mathematical calculations (binomial coefficients, hypergeometric functions, the Pochhammer symbol) are performed. All these services are used by the 'top level' one, which outputs values of dipole matrix elements between hydrogenic and Sturmian radial components to output the effective oscillator strengths averaged over the continuum included in a Gaunt factor generator of special value for integrated and spectrally-resolved bremsstrahlung and free-bound continua. This gives a structured architecture for the web service.

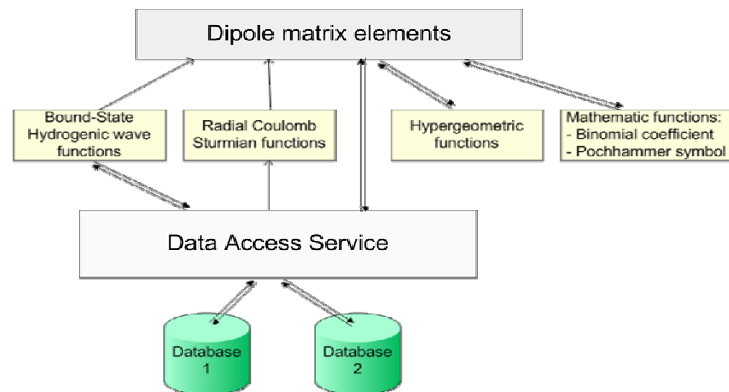


Figure 3. Web service approach for computing dipole matrix elements.

**2.2. Objective 2.:** Emission from the hydrogen atoms as related to the modelling of the RFP Extrap T2R plasma

### 2.3. Achievements

- Recombination and bremsstrahlung power loss in the Extrap T2R reversed field pinch (milestone completed)

Work on the interpretation of the hydrogen emission in the Extrap T2R plasma device has started since 2004, under collaboration with the Association EURATOM/VR, on the use of ADAS atomic package program. From the experimental investigation reported by the Swedish team one interesting aspect have been extracted: the fraction of total radiative power loss coming from the hydrogen bremsstrahlung and how much of the continuum comes from recombination to various impurity ions present in the plasma. The ionization per photon coefficient that relates the emission in a spectrum line integrated along a line of sight directed at a localized surface to the flux of ions from the surface has been calculated for different Balmer series lines. The charge exchange and ion-impact excitation transition with  $\Delta n = 0$  in hydrogen-hydrogen reactions were been considered to output the population density distribution on the  $n$  shell. Separate account was taken for  $H + O^+$  charge exchange process.

- Radiated power and impurity concentrations in the Extrap T2R reverse field pinch [10](milestone completed)

Results refer to the bremsstrahlung contribution to the total radiated power in form of the emission coefficient (in photons/sr/  $\text{\AA}/\text{cm}^2$  units) versus wavelength (in  $\text{\AA}$  units) for hydrogen series lines into the plasma. Data have been included into total radiative power loss and impurities concentration calculation for the Extrap T2R plasma device.

### 3. Conclusions

The work which has been undertaken in 2005 was focused on the analysis of discrepancies between  $Z_{\text{eff}}$  values as given from visible bremsstrahlung and charge exchange recombination spectroscopy. It has been improved by additional calculation on bound-free and free-free transitions in complex atomic system. New method to evaluate the corresponding Gaunt factors has been proposed.

A special attention has been paid to the accuracy of atomic data supplied by ADAS. Results on  $\Delta n=2$  dielectronic recombination channel in Li-like into Be-like C was first time reported. The iso-electronic sequence of Li-like ions has been analyzed and the consequences on the rate coefficients were been discussed.

Atomic data for , the atomic data for tungsten ions belonging to Ba-like, Ca-like, Hf-like, Sr-like and Zn-like iso-electronic sequences have been provided and reported.

Web service for remote atomic data access has been proposed and distributed applications were been pointed out.

### 4. Expected results for 2006

The following milestones will continue during 2006:

- Comparative studies from CXR and VB on the JET plasma taking full account of the contribution from resonances to the rate coefficients for many transitions



in complex ions having open 3d shells; Data from CXS will be analyzed with respect to the contribution from Zn-like tungsten ions.(Collaboration with TF-D)

- Atomic data for complex atoms with 3d open shell will be provided on the basis of the close-coupling method. e.g. R-matrix calculation(RMATXII) including relativistic effects and configuration interaction.(Collaboration with The Queen's University of Belfast)
- Web service for remote atomic data access will be implemented on atomic server, to make possible distributed applications and collaborative work between different groups belonging to different Associations interested to use our computer facility.
- Relative contribution to the line intensity coming from CXR and excitation rates in the Extrap T2R plasma related to the plasma edge characterization and modelling.

### References

[1] **Stancalie V., and JET EFDA contributors**, “*New Method to Calculate the Gaunt factor for the Refinement of  $Z_{\text{eff}}$  Evaluation in Fusion Plasmas*”, EFDA-JET-CP(05)02-49

[2] **Chelmus A.R.D., Stancalie V.**, “*Radiative Gaunt Factors*“, Journal of Optoelectronics and Advanced Materials, 7(2005)2405.

[3] **Stancalie V.**, “ *$1s^2 2pns(^1P^0)$  autoionizing levels in Be-like Al and C ions*”, Physics of Plasmas 12, 043301(2005)

[4] **Stancalie V.**, “*Complements to nonperturbative treatment of radiative damping effect in dielectronic recombination:  $\Delta n = 2$  transition in C IV*”, Physics of Plasmas 12, 100705(2005)

[5] **Stancalie V., Pais V., Mihailescu A., Chelmus A.R.D.**, “*Effective collision strengths for electron impact excitation in  $Al^{10+}$* ”, presented at the 32<sup>nd</sup> EPS Conference on Plasma Physics, 8<sup>th</sup> International Workshop on Fast Ignition of Fusion Targets, Tarragona, 27<sup>th</sup> June – 1<sup>st</sup> July, 2005.

[6] **Stancalie V., Burke V.M., Burke P.G., Hibbert A., Scott M.P.**, “*Electron impact excitation of complex atoms and ions: Forbidden transitions in  $Co^{3+}$* ”, Submitted J. Phys. B.:At. Mol. Opt. Phys. (December, 2005)

[7] **Mihailescu A., Stancalie V., Pais V., Chelmus A.R.D.** “*Atomic data for Zn-like W ion as related to the plasma modelling*”, presented at the 32<sup>nd</sup> EPS Conference on Plasma Physics, 8<sup>th</sup> International Workshop on Fast Ignition of Fusion Targets, Tarragona, 27<sup>th</sup> June – 1<sup>st</sup> July, 2005.

[8] **Mihailescu A., Stancalie V.**, “*Complex atoms modelling for plasma diagnostics*”, Journal of Optoelectronics and Advanced Materials 7(2005)2413.

[9] **Pais V., Stancalie V.**, “*Using Web Services for Remote Data Access and Distributed Applications*”, presented at the 5<sup>th</sup> IAEA Technical Meeting on Control, data Acquisition, and remote Participation for Fusion Research, Budapest, Hungary, July 12 – 15, 2005.

[10] Corre Y., Rachlew E., Ceconello M., Gravestijn R.M., Hedqvist A., Pégourié B., Schunke B., and Stancalie V., “Radiated power and impurity concentrations in the Extrap-T2R reversed-field pinch”, Physica Scripta 71(2005)523.

#### 4. Collaborative actions

- Collaborative research on the plasma edge characterization and modelling, under the key area “Simulation of the VUV spectra from the reversed field pinch Extrap T2R plasma”

Between Association EURATOM/MEdC and Association EURATOM/VR has been concentrated towards hydrogen, the continuum and the series limit, the recombination spectrum (the volume recombination)-and the accurate measurements of fluxes which are derived from absolute intensities. With respect to this task a specific milestone was included as collaborative action: Study of Hydrogen Balmer series emission as related to the effect of dynamic and static ion fields on population picture.

Atom in plasma ion field is assumed to lie in a constant Stark electric field produced by the almost stationary ions, which splits the degenerate levels. This is then further averaged over the ion field probability distribution function to produce a broadened spectrum. The static field yields an ionization lifetime. Dynamics fields created by ions moving inside the Debye sphere around the neutral atom fit into the framework of collisional theory and may be treated as rate coefficients in population equations. It was an objective of this work to incorporate this consistently into the population picture and hence diagnose temperature and densities (Figure 4). Results refer to the interpretation of the hydrogen emission using ADAS checking the  $H_\alpha/H_\beta/H_\gamma$  ratios with predictions. Unfortunately, it has not been observed limit of the Balmer series, as predicted. However, one interesting aspect that has been extracted from these experiments was how large fraction of total radiative power comes from the hydrogen bremsstrahlung [10], how much of the continuum comes from recombination to various impurity ions present in the plasma. This milestone was completed.

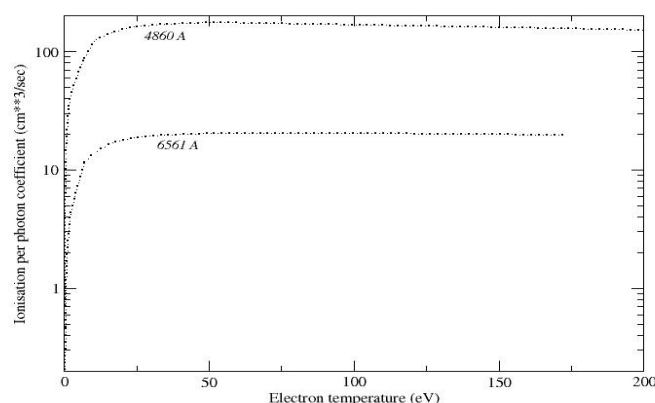


Figure 4. Ionisation per photon coefficient (in  $\text{cm}^3\text{s}^{-1}$  units) vs. electron temperature (eV units) for two Balmer series lines at  $4860\text{\AA}$  and  $6561\text{\AA}$ . The electron density is set to  $10^{13}\text{cm}^{-3}$ . The Extrap T2R is a medium sized device. The maximum values of the plasma parameters are: central ion temperature,  $T_i=0.25\text{KeV}$ , central electron temperature,  $T_e=0.3\text{KeV}$ , line averaged plasma density  $\langle n \rangle = 0.3 \times 10^{20}\text{m}^{-3}$ , plasma current,  $I=0.15\text{MA}$ , discharge pulse duration,  $0.025\text{ s}$ , energy confinement time,  $\tau_E = 0.00025\text{s}$ .

- Collaborative research on the specific objective “Reconciliation between the two methods (VB and CXS) of measuring  $Z_{\text{eff}}$  on JET and technique for keeping both diagnostics system synchronized

Between Association EURATOM/MEdC and Task Force D at JET site, included the following specific milestone: “Atomic data for complex atoms with two electrons outside closed shell ( $W^{18+}$ ,  $W^{54+}$ ). Due to the high temperature in the plasma, the tungsten ions reach high ionization stages and the radiation of the element occurs mainly in the far ultraviolet (VUV), extreme ultraviolet (EUV) and X ray regions. Heavy species such as tungsten have a complex spectra and thus, their calculation requires a much larger quantity of atomic data. Work which has been undertaken [8] reported atomic data for tungsten ions belonging to Ba-like, Ca-like, Hf-like, Sr-like iso-electronic sequences. The calculations were performed on the basis of the Cowan’s code in Hartree-Fock method including relativistic effects. The code computes spin-orbit parameter from the central-potential formula and also via the Blume-Watson method. The latest method gives more accurate values for atomic parameters. This milestone is completed.